Influence of higher harmonics on Poincaré maps derived from current self-oscillations in a semiconductor superlattice

K. J. Luo,* H. T. Grahn, S. W. Teitsworth,† and K. H. Ploog
Paul-Drude-Institut für Festkörperelektronik, Hausvogteiplatz 5-7, D-10117 Berlin, Germany
(Received 29 June 1998)

The effect of higher harmonics on the shape of Poincaré maps (first return maps) derived from current self-oscillations has been investigated in a semiconductor superlattice system driven by a dc + ac voltage bias. In addition to the intrinsic fundamental frequency, a number of higher harmonics with comparable amplitude are observed. The current oscillation traces are simulated according to the power spectra in order to determine the effect of the higher harmonics on the Poincaré maps. The calculated Poincaré maps for quasiperiodic oscillations as well as frequency locking are clearly distorted by the presence of the higher harmonics. The shape of the distorted Poincaré maps agrees with the experimentally observed ones. The calculation also reveals that the phase shift between the different frequency components of the current has an important effect on the shape of the Poincaré maps. [S0163-1829(98)03843-0]

The dynamical behavior in a variety of nonlinear systems can be described by a set of coupled, ordinary differential equations, which contain n variables. The time evolution of these variables constitutes a trajectory through an n-dimensional phase space.[1–3] It is usually possible and useful to analyze the dynamical behavior by making a transverse cut through the trajectory so that instead of a complex curve in the n-dimensional space one now has a set of points on an $(n-1)$-dimensional hypersurface, which is called the Poincaré map (or Poincaré section).[1–4] In a computer study of the dynamical behavior in an n-dimensional space, it is possible to analyze directly the n-dimensional signal. By contrast, in a physical experiment, one monitors typically only one scalar variable, e.g., the current response $I(t)$ for a system under a driving voltage. In this case, one usually records the first return map to analyze the attractors in a dissipative system. Taking the current response $I(t)$ as an example, the first return map is constructed by plotting I_{n+1} vs I_n, where I_n is sampled at a fixed phase in the nth period of the driving voltage.[5] The attractor revealed by the first return map may not be identical to the one in the Poincaré section; however, the first return map retains the same topological properties as the Poincaré section, which is sufficient to study the essential characteristics of the attractors.[1,3] In this paper, we will refer to the first return map as the Poincaré map.

The Poincaré map technique provides a natural link between continuous trajectories and discrete maps and makes it more convenient to analyze as well as visualize the attractors.[1,2] If the intrinsic oscillation contains no higher harmonics, the Poincaré map for frequency locking consists of a set of discrete points, while for quasiperiodicity it will be a simple smooth loop. In systems, where the motion of a space-charge layer determines the oscillation properties, higher harmonics are frequently present[5–10] because the space-charge layer is usually strongly localized within the sample. To the best of our knowledge, there has been no report about the distortion of Poincaré maps through the presence of higher harmonics up to now, although higher harmonics are clearly present in several solid-state systems.[5–10] In one particular case, the higher harmonics were removed using a filter.[6]

In the present investigation, the Poincaré maps derived experimentally for the current self-oscillations in a weakly coupled semiconductor superlattice (SL) system are found to be significantly distorted by the presence of higher harmonics. Even for quasiperiodicity, the Poincaré map can show a very complex structure. The current self-oscillations are simulated according to their power spectra, and the respective Poincaré maps are calculated. The simulated results do not agree with the experimentally derived ones, unless higher harmonics are included. The calculation also reveals that the phase shift between different frequency components has an important effect on the actual shape of the Poincaré maps.

The investigated sample consists of a 40-period, weakly coupled SL with 9.0-nm GaAs wells and 4.0-nm AlAs barriers grown by molecular beam epitaxy on a (100) n^+-type GaAs substrate. The central 5 nm of each well are n doped with Si at 3.0×10^{17} cm^{-3}. The SL is ''sandwiched'' between two highly Si-doped $Al_{0.5}Ga_{0.5}As$ contact layers forming an n^+-n-n^+ diode. The sample is etched to yield mesas with a diameter of 120 μm. The experimental data are recorded in a He-flow cryostat at 5 K using high-frequency coaxial cables with a bandwidth of 20 GHz. The driving voltage is generated with a Wavetek 50-MHz pulse/function generator (model 81). The power spectra of the current oscillations are detected with an Advantest R3361 spectrum analyzer. The real-time current traces are recorded with a Hewlett-Packard 54720A digital oscilloscope, which is triggered by the synchronization signal from the pulse/function generator using a sampling rate of 1 G samples/second and 32 768 points/snapshot. The resulting time resolution is about 50 points per period τ_d of the driving frequency, which corresponds to about $600\tau_d$ per snapshot.

Current self-oscillations in weakly coupled semiconductor superlattices originate from a recycling motion of a charge accumulation layer inside the superlattice.[11] For a dc bias fixed at 7.08 V, the intrinsic fundamental frequency (f_1) of the current self-oscillations is 11.4 MHz. In the experiment, the driving frequency (f_d) is set to the golden mean $(1+\sqrt{5})/2=1.618$ times f_1, i.e., 18.4 MHz, while the driving

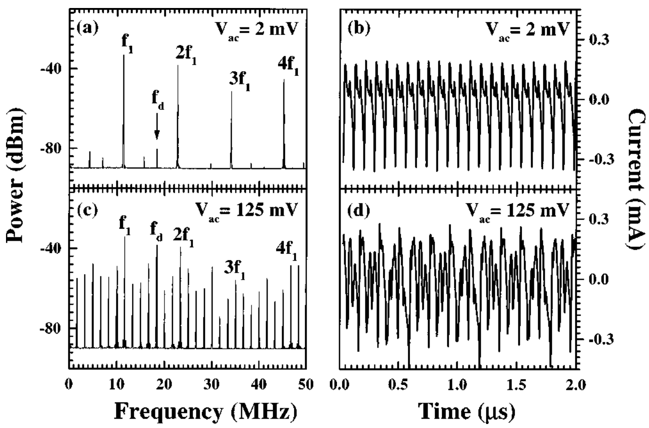

FIG. 1. Current power spectra (left) and real-time current traces (right) for $V_{ac}=2$ and 125 mV, respectively, recorded at 5 K in a superlattice structure.

amplitude (V_{ac}) is varied. At $V_{ac}=0$, the current oscillations contain up to three higher harmonics with a significant amplitude, which are clearly identified in the power spectra. When the driving voltage is applied, combination frequencies of the form nf_d+mf_1, where n and m are integers, also appear in the power spectrum in addition to f_1 and its higher harmonics.[10,12] Figure 1 shows the power spectra on the left and real-time current traces $I(t)$ on the right for two different values of V_{ac}. At 2 mV, the oscillation is quasiperiodic, since f_1 and f_d are incommensurate.[2,10,12] With increasing V_{ac}, f_1 will gradually shift to higher frequencies. At 125 mV, the frequency ratio f_1/f_d reaches a rational number with a value of 7/11, which is called the winding number. The system has now entered a so-called frequency-locked state.[2,10,12]

Figure 2(a) shows the Poincaré map derived from the real-time trace in Fig. 1(b) for $V_{ac}=2$ mV with the sampling phase fixed at the maximum of the amplitude of the driving voltage. As mentioned above, if there are no higher harmonics, the Poincaré map for quasiperiodic oscillations should be a smooth loop. This is obviously not the case in Fig. 2(a), where the Poincaré map is a distorted loop containing self-crossings. In the following, we will simulate the current traces by using sinusoidal functions in order to derive Poincaré maps for different conditions, which can be compared to the one obtained from the experimental data. The simulated results demonstrate that the distortion of the loop is caused by the presence of higher harmonics.

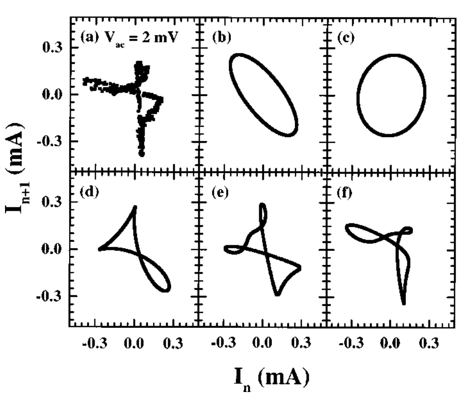

FIG. 2. (a) Experimentally derived Poincaré map for the quasiperiodic oscillations observed at 2 mV. Calculated Poincaré maps for (b) the fundamental frequency f_1 alone, (c) the second harmonic f_2 alone, (d) f_1 and f_2 together, (e) f_1 plus three higher harmonics and no phase shift ($\phi_1=0$), and (f) f_1 plus three higher harmonics and a phase shift of $\phi_1=0.8\pi$. The frequency ratio was set to $f_d/f_1=(1+\sqrt{5})/2$.

As a first approximation, we calculate the Poincaré maps at 2 mV without taking into account any higher harmonics. The driving voltage $V_d(t)$ is defined as

$$V_d(t)=V_{ac}\sin(\omega_d t), \tag{1}$$

where $\omega_d=2\pi f_d$. In the simplest case, the real-time current response $I(t)$ consists of two terms

$$I(t)=I_d\sin(\omega_d t)+I_1\sin(\omega_1 t+\phi_1), \tag{2}$$

where $\omega_1=2\pi f_1$. The first term represents the response due to the driving voltage, which has the same frequency and phase as the driving voltage. The second term denotes the intrinsic current component, which exhibits a phase shift ϕ_1 with respect to the driving voltage.

In the power spectra, the measured quantity $P(f)$ is defined as

$$P(f)=10\log_{10}[|I(f)|^2], \tag{3}$$

where $I(f)$ denotes the amplitude of the oscillatory component with frequency f. In the measured power spectra, the current amplitude is converted into a voltage. In the following, only amplitude ratios are important, and the current amplitude in the calculation has been normalized to an arbitrary constant. From the power spectra in Fig. 1(a), we can determine the amplitude ratio between the driving and intrinsic frequency components. In the calculation, we have used a value of 229 for I_1/I_d. As mentioned above, the frequency ratio f_d/f_1 was set at $(1+\sqrt{5})/2$. The current traces are calculated using Eq. (2) with a time scale adjusted in such a way that every Poincaré map contains about 500 data points. Figure 2(b) shows the calculated Poincaré map using the parameters given above with a phase shift $\phi_1=0$, which consists of a smooth loop. Changing the value of ϕ_1 does not result in any changes of the shape of the Poincaré map, although the exact location of the points in the Poincaré map may be influenced. Therefore, we conclude that, if higher harmonics are not taken into account, the phase difference between the driving and intrinsic frequency components does not have any effect on the shape of the Poincaré map. However, the calculated result in Fig. 2(b) is very different from the experimentally observed result shown in Fig. 2(a). In a previous paper,[12] we have studied the Poincaré map for certain dc voltages, where the current response in the quasiperiodic regime does not contain any higher harmonics. Then, the resulting Poincaré map is indeed very similar to the one shown in Fig. 2(b). In contrast, when the higher harmonics are experimentally present as shown in Figs. 1(a) and 1(c), it is necessary to include them in the simulation.

Figure 2(c) shows the calculated Poincaré map for the second harmonic alone, which corresponds to the Poincaré map for a frequency ratio of $(1+\sqrt{5})/4$. It is again a smooth loop without any distortion, but has a different shape than the one in Fig. 2(b). Any phase shift has again no effect on the shape. However, when at least the fundamental frequency and the second harmonic are considered according to

$$I(t)=I_d\sin(\omega_d t)+I_1\sin(\omega_1 t+\phi_1)+I_2\sin(2\omega_1 t+\phi_2), \tag{4}$$

where I_2 denotes the amplitude of the second harmonic, the loop becomes already distorted containing at least one self-crossing. This is shown in Fig. 2(d) for $\phi_1=\phi_2=0$. The amplitude ratios $I_1/I_d=229$ and $I_2/I_d=126$ have been determined from the power spectra at 2 mV.

In order to improve the simulated result with respect to the experimentally observed one, the Poincaré map is now derived from a current response that includes all three higher harmonics shown in Fig. 1(a). We therefore consider at 2 mV a current response of the form

$$I(t)=I_d\sin(\omega_d t)+I_1\sin(\omega_1 t+\phi_1)+I_2\sin(2\omega_1 t+\phi_2)+I_3\sin(3\omega_1 t+\phi_3)+I_4\sin(4\omega_1 t+\phi_4), \tag{5}$$

where I_3 and I_4 denote the amplitudes of the third and fourth harmonic, respectively. A total of five frequencies is now taken into account. The other frequency peaks, which are present in Fig. 1(a) and originate from the mixing of f_1 with f_d, are not included in Eq. (5), since their amplitudes are rather small. We also confirmed that they have little influence on the calculated results. From the power spectra at 2 mV, the additional amplitude ratios used in the calculation have been determined to be $I_3/I_d=28$ and $I_4/I_d=45$. For simplicity, we assume that there is no phase shift between the fundamental intrinsic frequency and its higher harmonics, i.e., $\phi_1=\phi_i$ for $i=2,3$, and 4. However, the phase shift between the driving frequency and all other frequencies may still have an important effect on the shape of the Poincaré map.

Figure 2(e) shows the calculated Poincaré map when all three higher harmonics of Fig. 1(a) are included with a phase shift $\phi_1=0$. Comparing it with Fig. 2(d), the number of self-crossings increases when more higher harmonics are taken into account. We tried a number of different values for ϕ_1. The best qualitative agreement in terms of the shape of the Poincaré map was found for a value of 0.8π as shown in Fig. 2(f). This clearly demonstrates the influence of higher harmonics on the shape of the Poincaré map. The remaining difference between Figs. 2(a) and 2(f) may originate from a phase shift between the different frequency components in the current traces. Better agreement can be expected, if the phase shifts are finely tuned between the different frequency components. In principle, they can be obtained from complete Fourier transforms of the corresponding real-time traces. However, the effect of higher harmonics and phase shifts on the Poincaré maps can already be demonstrated using the procedure outlined above.

We will now calculate the Poincaré map for the frequency-locked state observed at 125 mV in the same way as described above. The Poincaré map is expected to contain 11 separate points, since the winding number is equal to 7/11.[12] The experimental result is shown in Fig. 3(a) and consists of some 10 isolated areas. However, it appears that one of the longer regions actually consists of two separate regions. Figure 3(b) displays the calculated Poincaré map without considering any higher harmonics, i.e., the current

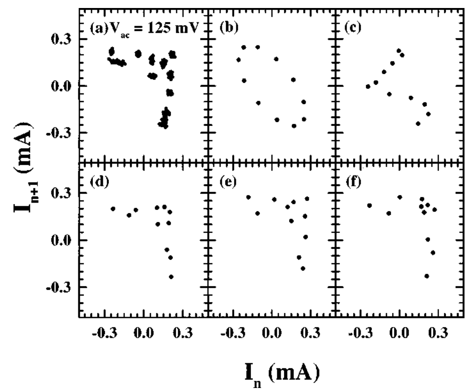

FIG. 3. (a) Experimentally derived Poincaré map for frequency locking observed at 125 mV corresponding to a winding number of 7/11. Calculated Poincaré maps for a frequency ratio of $f_1/f_d=7/11$ (b) without considering any higher harmonics of f_1, (c) including three higher harmonics and no phase shift ($\phi_1=0$), (d) including three higher harmonics with the same phase shift of $\phi_1=0.8\pi$, (e) including all higher frequency components with a phase shift of $\phi_1=0.8\pi$, and (f) including all higher frequency components with phase shifts of $\phi_1=0.8\pi$ for the three higher harmonics and $\phi_1=0$ for all the other frequency components.

trace has been simulated using Eq. (2) with a frequency ratio of $f_d/f_1=11/7$. It indeed contains 11 isolated points along a similar loop as that shown in Fig. 2(b). It should be noted that there are 500 data points inside a single Poincaré map so that each isolated point actually consists of about 45 points, which have exactly the same value. The calculated result in Fig. 3(b) is again very different from the experimental result so that higher harmonics have to be taken into account.

Just as in the calculation for 2 mV, we simulate the current trace using Eq. (5). The amplitude ratio of I_i/I_d for $i=1,2,3$, and 4 is again obtained from the power spectra with values of 1.40, 0.70, 0.15, and 0.28, respectively. We also assume no phase shift between the f_1 component and the f_i ($i=2,3,4$) components. Figures 3(c) and 3(d) display the calculated results for a phase shift between the driving and intrinsic frequency component of $\phi_1=0$ and $\phi_1=0.8\pi$, respectively. The agreement between the experimental and simulated result is greatly improved in Fig. 3(d) compared with Fig. 3(c). However, it may be further improved by taking into account all other frequency peaks (there are 24) shown in Fig. 1(c), which are linear combinations of f_d and f_1. In contrast to the quasiperiodic case at 2 mV, these frequency peaks are rather strong [cf. Fig. 1(c)]. In Fig. 3(e), the corresponding Poincaré section is shown under the assumption that the phases of all terms are set to 0.8π, i.e., there is no relative phase shift between any of these terms. Compared with that in Fig. 3(d), the overall shape in Fig. 3(e) has only changed a little, but some details are in better agreement with the experimental result. In particular, the lowest two points are now very close to each other indicating that the large region in the lowest part of Fig. 3(a) actually consists of two regions, which are connected.

Figure 3(f) shows the calculated Poincaré map including all frequency components assuming a different phase shift from that in Fig. 3(e). The phase shift for the intrinsic frequency and its higher harmonics is the same as for Fig. 3(e), but for all other frequency components (i.e., the mixing terms) the phase has been set to zero. Again, the overall shape does not change very much, but the separation distance between the different points is varied. Among the simulated results for the frequency-locked state, Fig. 3(e) shows the best agreement with the experimental Poincaré map. Therefore, we conclude that also for the frequency-locked state the presence of the higher harmonics and mixed frequency components result in a distortion of the Poincaré map. A detailed reproduction of the experimentally observed shape can only be achieved by including nonzero phase shifts between the different frequency components.

In summary, the effect of the higher harmonics on the shape of Poincaré maps has been investigated for a driven semiconductor superlattice, where the current self-oscillations originate from a recycling motion of a charge accumulation layer. Experimental results show that the Poincaré maps are significantly distorted by the presence of higher harmonics. Even for quasiperiodic oscillations and frequency locking, the Poincaré maps show a rather complicated structure. The simulation including the higher harmonics and taking into account finite phase shifts between the different frequency components reproduces the main features of the experimental results. Therefore, Poincaré maps contain information about the presence of higher harmonics and the phase shift between these frequency components.

The authors would like to thank A. Fischer for sample growth. Partial support of the Deutsche Forschungsgemeinschaft within the framework of Sfb 296 is gratefully acknowledged.

*Electronic address: kjluo@pdi-berlin.de

†Permanent address: Department of Physics, Duke University, Box 90305, Durham, NC, 27708-0305.

[1] P. Bergé, Y. Pomeau, and C. Vidal, *Order Within Chaos* (Wiley & Sons, New York, 1984).

[2] M. P. Shaw, V. V. Mitin, E. Schöll, and H. L. Grubin, *The Physics of Instabilities in Solid State Electron Devices* (Plenum, New York, 1992), Chap. 1.

[3] E. Ott, *Chaos in Dynamical Systems* (Cambridge University Press, New York, 1993).

[4] J.-P. Eckmann and D. Ruelle, Rev. Mod. Phys. **57**, 617 (1985).

[5] O. M. Bulashenko and L. L. Bonilla, Phys. Rev. B **52**, 7849 (1995); O. M. Bulashenko, M. J. García, and L. L. Bonilla, *ibid.* **53**, 10 008 (1996).

[6] G. A. Held and C. Jeffries, Phys. Rev. Lett. **55**, 887 (1985).

[7] A. M. Kahn, D. J. Mar, and R. M. Westervelt, Phys. Rev. B **46**, 7469 (1992).

[8] *Nonlinear Dynamics and Pattern Formation in Semiconductors and Devices*, edited by F.-J. Niedernostheide (Springer-Verlag, Berlin, 1995), Chaps. 8 and 10.

[9] M. J. Bergmann, S. W. Teitsworth, L. L. Bonilla, and I. R. Cantalapiedra, Phys. Rev. B **53**, 1327 (1996).

[10] Y. Zhang, J. Kastrup, R. Klann, K. H. Ploog, and H. T. Grahn, Phys. Rev. Lett. **77**, 3001 (1996); Y. Zhang, R. Klann, H. T. Grahn, and K. H. Ploog, Superlattices Microstruct. **21**, 565 (1997).

[11] J. Kastrup *et al.*, Phys. Rev. B **55**, 2476 (1997).

[12] K. J. Luo, H. T. Grahn, K. H. Ploog, and L. L. Bonilla, Phys. Rev. Lett. **81**, 1290 (1998).